

Vacuum structure of Carbon Nanotube Torus

K. Sasaki

Department of Physics, Tohoku University, Sendai 980-8578, Japan

Low energy excitations in carbon nanotubes can be described by an effective field theory of two components spinor. It is pointed out that the chiral anomaly in 1+1 dimensions should be observed in a metallic carbon nanotube torus on a planar geometry with varying magnetic field. We propose an experimental setup for studying this quantum effect. We also analyze the vacuum structure of the metallic carbon nanotube torus including the Coulomb interactions and discuss some effects of external charges.

I. INTRODUCTION

In recent years carbon nanotubes(CNTs) [1] have attracted much attention from various points of view. Especially their unique mechanical and electrical properties have stimulated many people's interest in the analysis of CNTs [2,3]. They have exceptional strength and stability, and they can exhibit either metallic or semiconducting depending on diameter and helicity [4,5]. Because of their small size, properties of CNTs should be governed by the law of quantum mechanics. Therefore it is quite important to understand the quantum behavior of the electrons on CNTs. The bulk electric properties of (single-walled)CNTs are relatively simple, but the behavior of electrons at metal-CNT junction is complicated and its understanding is necessary for building actual electrical devices. On the other hands, a CNT torus (Fullerene 'Crop Circles' [6]) is clearly simple because of its no-boundary shape and it can also be either metal or semiconducting. Even in the torus case, quite important effect: 'chiral anomaly' [7], which is of essentially quantum nature, might occur.

Low energy excitations on CNTs at half filling move along the tubule axis because the circumference degree of freedom (an excitation in the compactified direction) is frozen by a wide energy gap. Hence this system can be described as a 1+1 dimensional system. Furthermore in the case of metallic CNTs, the system describing small fluctuations around the Fermi point is equivalent to the chiral(massless) fermion in 1+1 dimensions. If we include gauge field, this situation can be modeled by the quantum field theory of chiral fermion which couples to the gauge field through minimal coupling. This model realizes the chiral anomaly phenomenon [8]. In this paper, we examine the anomaly effect in a metallic carbon nanotube torus and discuss how such an effect can be observed experimentally. We also clarify the vacuum structure of this model regarding the gauge field as a classical field and discuss some effects of external charges situated on the metallic CNT torus.

The organization of this paper is as follows. After reviewing quantum physics of CNTs [9], we study the case of CNT torus in section II. In section III we point out that low energy excitations on a metallic CNT torus at half filling can be modeled by a quantum field theory of chiral fermions with gauge field and construct the Hamiltonian of this system. In section IV we discuss the chiral anomaly and show how such effect can be observed experimentally. We examine the Hamiltonian including the Coulomb interactions and analyze an effect of the Coulomb interactions on the chiral anomaly in section V. We discuss some effects of external charges in section VI. Conclusion and discussion are given in section VII.

II. CARBON NANOTUBE TORUS

A carbon nanotube can be thought of as a layer of graphite sheet folded-up into a cylinder. A Graphite sheet consists of many hexagons whose vertices are occupied by the carbon atoms and each carbon supplies one conducting electron which determines the electric properties of the graphite sheet. The lattice structure of a two-dimensional graphite sheet is shown in Fig.1.

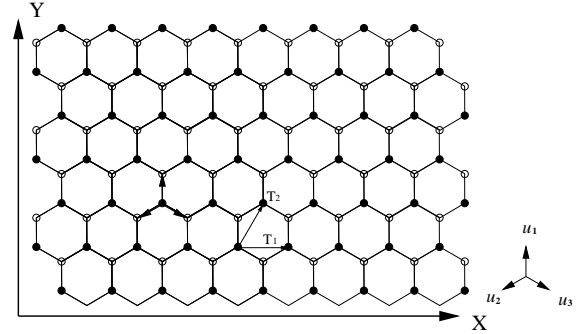


FIG. 1. Lattice structure of a two-dimensional graphite sheet ($u_1 = ae_y$, $u_2 = -\frac{\sqrt{3}}{2}ae_x - \frac{1}{2}ae_y$, $u_3 = \frac{\sqrt{3}}{2}ae_x - \frac{1}{2}ae_y$)

It is obvious, however, that this picture of a CNT as a graphite sheet rolled up to form a compact cylinder is somewhat oversimplified. We need to be careful of the following facts. First, a conducting electron makes π orbital whose wave function extends into the Z-direction: perpendicular to the graphite sheet. Hence, in the case of multi-walled CNTs(MWCNTs), the wave functions which belong to different layers may interfere so that there is a chance that some electrical properties will alter [10]. Second, we should care for the curvature of a cylinder. This cause the mixing of σ and π orbital so that the band structure might change. In the present

paper, we concentrate single-walled CNTs with a large diameter. Therefore the effects of interlayer interactions and curvature can safely be neglected.

There are two symmetry translation vectors on the planar honeycomb lattice,

$$T_1 = \sqrt{3}ae_x, \quad (2.1)$$

$$T_2 = \frac{\sqrt{3}}{2}ae_x + \frac{3}{2}ae_y. \quad (2.2)$$

Here a denotes the length of the nearest carbon vertex. e_x and e_y are unit vectors which are orthogonal to each other ($e_x \cdot e_y = 0$). If we neglect the spin degrees of freedom, because of these symmetry translations, Hilbert space is spanned by the following two Bloch basis vectors,

$$|\Psi_{\bullet}^k\rangle = \sum_{i\bullet} e^{ikr_i} a_i^\dagger |0\rangle, \quad (2.3)$$

$$|\Psi_{\circ}^k\rangle = \sum_{i\circ} e^{ikr_i} a_i^\dagger |0\rangle, \quad (2.4)$$

where the black(\bullet) and blank(\circ) indices are indicated in Fig.1. r_i labels the vector pointing each site i , and a_i, a_j^\dagger are canonically annihilation-creation operators of the electrons of site i and j ,

$$\{a_i, a_j^\dagger\} = \delta_{ij}. \quad (2.5)$$

We construct a state vector which is an eigenvector of these symmetry translations as follows:

$$|\Psi^k\rangle = C_{\bullet}^k |\Psi_{\bullet}^k\rangle + C_{\circ}^k |\Psi_{\circ}^k\rangle. \quad (2.6)$$

In order to define the unit cell of wave vector k , we act the symmetry translation operators on the state vector and obtain the first Brillouin zone

$$-\frac{\pi}{\sqrt{3}} \leq ak_x < \frac{\pi}{\sqrt{3}}, \quad -\pi \leq \frac{\sqrt{3}}{2}ak_x + \frac{3}{2}ak_y < \pi, \quad (2.7)$$

where $k_x = k \cdot e_x$.

The mapping of the graphite sheet onto a cylindrical surface is specified by a wrapping vector:

$$C = NT_1 + MT_2, \quad (2.8)$$

which defines the relative location of the two sites. The pair of indices (N, M) describes how the sheet is wrapped to form the cylinder, and determines its electrical properties [4,5]. It can be divided CNTs into three categories depending on the pair of integers (N, M) . A tube is called ‘zigzag’ type if $M = 0$ and ‘armchair’ in the case $M = -2N$. All other tubes are of the ‘chiral’ type.

To study the electronic properties of a CNT torus quantum mechanically, first we compactify the graphite sheet into a cylinder by imposing a periodic boundary condition to the state vector. In general, we may consider the following boundary condition,

$$\hat{G}(NT_1 + MT_2)|\Psi^k\rangle = |\Psi^k\rangle. \quad (2.9)$$

\hat{G} denotes a symmetry translation operator. From which we obtain

$$\frac{\sqrt{3}}{2}(2N + M)ak_x + \frac{3}{2}Mak_y = 2\pi n, \quad (2.10)$$

where n is an integer. Next, in order to make a torus, we compactify the tube into a torus by imposing a boundary condition to the tubule axis direction. For example, we may consider a ‘zigzag torus’ which has the following boundary conditions,

$$\begin{aligned} \hat{G}(NT_1)|\Psi^k\rangle &= |\Psi^k\rangle, \\ \hat{G}(M(2T_2 - T_1))|\Psi^k\rangle &= |\Psi^k\rangle. \end{aligned} \quad (2.11)$$

The former condition makes a sheet into a zigzag tube, and the latter forces the tube into a zigzag torus.

It is clear that there are many possibilities for the shape of torus and each shape has its own boundary condition. So, some of them have different properties from the one (2.11). Especially we can imagine a CNT torus in which some twist exists along the tubule axis direction [11]. This system has the following boundary conditions,

$$\begin{aligned} \hat{G}(NT_1)|\Psi^k\rangle &= |\Psi^k\rangle, \\ \hat{G}(M(2T_2 - T_1))|\Psi^k\rangle &= \hat{G}(\tilde{N}T_1)|\Psi^k\rangle, \end{aligned} \quad (2.12)$$

where \tilde{N} is decided by the twist at the junction of tube end, see Fig.2. These boundary conditions yield the discrete wave vectors

$$ak_x = \frac{2\pi}{\sqrt{3}} \frac{n}{N}, \quad ak_y = \frac{2\pi}{3M} \left(m + \frac{\tilde{N}}{N} \right). \quad (2.13)$$

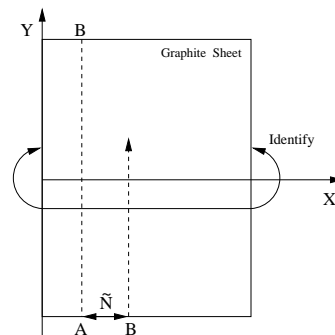


FIG. 2. Twisted zigzag torus: We impose the periodic boundary condition in the X-direction and attach same character(‘B’) in the Y-direction to obtain a twisted CNT torus. There are \tilde{N} hexagons between the point A and B.

So far we have constructed the Hilbert space of the conducting electrons. The Hilbert space is spanned by the Bloch basis vectors with the discrete wave vectors (2.13). Now, we consider the Hamiltonian which governs the time evolution of a state vector. Each carbon atom has an electron which makes π -orbital. The electron can

transfer from any site to the nearest three sites through the quantum mechanical tunneling or thermal hopping in finite temperature. Therefore there is some probability amplitude for this process. In this case, the tight-binding Hamiltonian is most suitable:

$$\mathcal{H} = E_0 \sum_i a_i^\dagger a_i + \gamma \sum_{\langle i,j \rangle} a_i^\dagger a_j, \quad (2.14)$$

where the sum $\langle i, j \rangle$ is over pairs of nearest-neighbors carbon atoms i, j on the lattice. γ is the transition amplitude from one site to the nearest sites and E_0 is the one from a site to the same site. This parameter E_0 only fixes the origin of the energy and therefore irrelevant. It is an easy task to find the energy eigenstates and eigenvalues of this Hamiltonian. In the matrix representation, the energy eigenvalue equation reads

$$\begin{pmatrix} E_0 & \gamma \sum_i e^{iku_i} \\ \gamma \sum_i e^{-iku_i} & E_0 \end{pmatrix} \begin{pmatrix} C_\bullet^k \\ C_\circ^k \end{pmatrix} = E_k \begin{pmatrix} C_\bullet^k \\ C_\circ^k \end{pmatrix}, \quad (2.15)$$

where

$$|\Psi_\bullet^k\rangle = \begin{pmatrix} 1 \\ 0 \end{pmatrix}, \quad |\Psi_\circ^k\rangle = \begin{pmatrix} 0 \\ 1 \end{pmatrix}, \quad (2.16)$$

and the vector u_i is a triad of vectors pointing respectively in the direction of the nearest neighbors of a black point, see Fig.1. The energy eigenvalues and eigenvectors are as follows,

$$E_k = E_0 \pm \Delta(k), \quad (2.17)$$

$$\begin{pmatrix} C_\bullet^k \\ C_\circ^k \end{pmatrix} = \frac{1}{\sqrt{2}\Delta(k)} \begin{pmatrix} \gamma \sum_i e^{iku_i} \\ \pm \Delta(k) \end{pmatrix}, \quad (2.18)$$

where

$$\Delta(k) = \gamma \sqrt{1 + 4 \cos \frac{\sqrt{3}}{2} a k_x \cos \frac{3}{2} a k_y + 4 \cos^2 \frac{\sqrt{3}}{2} a k_x}.$$

The structure of this energy band has striking properties when considered at half filling. This is the situation which is physically interesting. Since each level of the band may accommodate two states due to the spin degeneracy, the Fermi level turns out to be at midpoint of the band ($E_k = E_0$). Fermi points in the first Brillouin zone are located at

$$\tilde{k}_{1,2} = (a k_x, a k_y) = \left(\pm \frac{2\pi}{3\sqrt{3}}, \mp \frac{2\pi}{3} \right). \quad (2.19)$$

Hence, if N in eq.(2.13) is a multiple of 3, then the zigzag torus shows metallic properties.

In order to understand the electric properties we should take into account a small perturbation around the Fermi point. So we take $k = \tilde{k}_1 + \delta k$ as a small fluctuation [12]. Perturbation around the point \tilde{k}_2 is same as around the point $k = \tilde{k}_1$. So we may only consider one of the pairs. In this case the Hamiltonian which describes the system is given by [13]

$$-\frac{3}{2}\gamma\sigma \cdot \delta k = -\frac{3}{2}\gamma a \begin{pmatrix} 0 & \delta k_x - i\delta k_y \\ \delta k_x + i\delta k_y & 0 \end{pmatrix}. \quad (2.20)$$

This implies that the low energy excitations of metallic CNTs at half filling are described by an effective theory of two dimensional spinor obeying the Weyl equation. In coordinate space, we find

$$\mathcal{H}_{pert} = -\frac{3\gamma a}{2\hbar} \sigma \cdot p, \quad (2.21)$$

where p is the momentum operator, $p = -i\hbar\nabla$ and σ_i are the Pauli matrices. It is also convenient to use a parameter $\beta = -\frac{3\gamma a}{2\hbar}$ and $T = \beta t$. In this case the Schrödinger equation becomes

$$i\hbar \frac{\partial}{\partial T} \psi = (\sigma \cdot p) \psi. \quad (2.22)$$

In the following section, we consider metallic and semi-conducting zigzag torus that have small N and large M values ($\frac{M}{N} \sim 10^2$). In this case, transitions between different k_x are very small because of their costed energy ($\sim \frac{|\gamma|}{N}$) as compared to that of k_y : ($\sim \frac{|\gamma|}{M}$). Therefore, the only surviving degree is a motion in the tubule axis direction, i.e. this system is a 1+1 dimensional system effectively.

III. EFFECTIVE FIELD THEORY OF CARBON NANOTUBE

In this section we would like to focus on the zigzag torus which has the boundary conditions (2.11) and construct an effective field theory describing the low energy excitations in the torus. More general boundary conditions(2.12) are discussed in section IV. The zigzag torus can exhibit either metallic or semi-conducting depending on the value of N . If N is a multiple of 3 then the torus becomes metallic. In order to analyze the semi-conducting case equally, we set $N = \pm 3n + b$, where n is a positive integer and $b \in \{0, \pm 1, \pm 2\}$. To examine the low energy excitations, we should consider the following wave vectors and energy:

$$a k_x = \pm \frac{2\pi}{3\sqrt{3}} \frac{1}{1 \pm \frac{b}{3n}}, \quad a k_y = \mp \frac{2\pi}{3} + a \delta k_y, \quad (3.1)$$

$$E_k = E_k \left(\pm \frac{2\pi}{3\sqrt{3}} \frac{1}{1 \pm \frac{b}{3n}}, \mp \frac{2\pi}{3} + a \delta k_y \right). \quad (3.2)$$

Considering the small perturbation ($a\delta k_y < \frac{2\pi}{9}$) and a large diameter ($n > 3$), the excitation energy can be approximated by

$$E_k \sim \pm \beta \sqrt{M^2 + p^2}, \quad (3.3)$$

where $p = \hbar \delta k_y$ and

$$M = \frac{2\pi\hbar}{\sqrt{3}3na} \frac{b}{3}. \quad (3.4)$$

Consequently, we have obtained a linear dispersion relation for metallic case ($b = 0$). This is to be contrasted with the dispersion relation for semi-conducting case ($b \neq 0$).

Here we comment on the excitations between different k_x . In order to neglect these excitations, we have to restrict the energy to the following region:

$$E_k < E_{\delta k_x} = \frac{\sqrt{3}\pi}{N}\gamma. \quad (3.5)$$

At room temperature, thermal excitation between different $|\delta k_x|$ cannot occur by the Boltzmann suppression factor, $e^{-\frac{E_{\delta k_x}}{kT}} (\sim e^{-\frac{500}{N}})$, so that the effects of different $|\delta k_x|$ can be ignored. Accordingly, the Hamiltonian which describes the low energy excitations near the Fermi point is given by

$$-\frac{3}{2}\frac{\gamma a}{\hbar} \begin{pmatrix} 0 & \pm M - ip \\ \pm M + ip & 0 \end{pmatrix}. \quad (3.6)$$

The sign (\pm) in front of M comes from the \tilde{k}_1 and \tilde{k}_2 points. The sign can be removed by an appropriate unitary transformation of the state vector. Therefore we may choose the minus sign without loss of generality. Using the unitary transformation, $U = e^{-i\frac{\pi}{4}\sigma_x}$, the Schrödinger equation becomes

$$i\hbar \frac{\partial}{\partial T} \psi = \begin{pmatrix} p & -M \\ -M & -p \end{pmatrix} \psi. \quad (3.7)$$

One can obtain the quantum field theory by promoting the wave function (ψ) to the field operator (Ψ) obeying the anti-commutation relation. Because the Schrödinger equation (3.7) is the Dirac equation in two dimensions, it is appropriate to adopt the following Lagrangian density. Addition of the electro-magnetic interaction according to the minimal coupling gives

$$\mathcal{L} = -\frac{1}{4}F^{\mu\nu}F_{\mu\nu} - \bar{\Psi}(\not{D} + M)\Psi, \quad (3.8)$$

where \not{D} is the covariant derivative and $F_{\mu\nu}$ is the field strength,

$$\begin{aligned} \not{D} &= \sum_{\mu=0,1} \left(i\hbar\partial_\mu - \frac{e}{c}A_\mu \right) \gamma^\mu, \\ F_{\mu\nu} &= \partial_\mu A_\nu - \partial_\nu A_\mu. \end{aligned} \quad (3.9)$$

The gauge field lives in four dimensional space-time so that summation indices run from 0 to 3 in the gauge kinetic term. We adopt the following notation:

$$\begin{aligned} g^{\mu\nu} &= \text{diag}\{1, -1, -1, -1\}, \quad \gamma^0 = \begin{pmatrix} 0 & 1 \\ 1 & 0 \end{pmatrix}, \\ \gamma^1 &= \begin{pmatrix} 0 & 1 \\ -1 & 0 \end{pmatrix}, \quad \gamma^5 = -\gamma^0\gamma^1 = \begin{pmatrix} 1 & 0 \\ 0 & -1 \end{pmatrix}. \end{aligned} \quad (3.10)$$

We quantize the fermion field in each configuration of the gauge field choosing Weyl gauge condition. Fermionic part of the Hamiltonian density is given by

$$\mathcal{H} = \mathcal{H}_F + \mathcal{H}_C. \quad (3.11)$$

The total Hamiltonian density consists of the kinetic term and the Coulomb term. The kinetic term is given by

$$\begin{aligned} \mathcal{H}_F &= \Psi^\dagger h_F \Psi \\ &= \Psi^\dagger \begin{pmatrix} i\hbar\partial_1 - \frac{e}{c}A_1 & -M \\ -M & -(i\hbar\partial_1 - \frac{e}{c}A_1) \end{pmatrix} \Psi. \end{aligned} \quad (3.12)$$

The Coulomb interaction term is

$$\mathcal{H}_C = \frac{e^2}{8\pi} \int \frac{J^0(x)J^0(y)}{|x-y|} dy. \quad (3.13)$$

where $eJ^0(x)$ stands for the charge density. The electric current is given by $eJ^\mu = e\bar{\Psi}\gamma^\mu\Psi$ where e is the electron charge.

IV. CHIRAL ANOMALY IN THE METALLIC CARBON NANOTUBE TORUS

We have obtained the Hamiltonian density which describes the low energy excitations in the zigzag torus. The Hamiltonian consists of two parts, one is the kinetic term and the other is the Coulomb interaction. In this section we discuss the quantum mechanical vacuum structure of the kinetic Hamiltonian: $H_F (= \int \mathcal{H}_F)$. Effects of the Coulomb interaction will be considered in latter sections. Hereafter we focus on the metallic case. In the metallic case: $b = 0$, the energy eigenvectors are given by

$$\begin{aligned} h_F \psi_n \begin{pmatrix} 1 \\ 0 \end{pmatrix} &= \epsilon_n \psi_n \begin{pmatrix} 1 \\ 0 \end{pmatrix}, \quad h_F \psi_n \begin{pmatrix} 0 \\ 1 \end{pmatrix} = -\epsilon_n \psi_n \begin{pmatrix} 0 \\ 1 \end{pmatrix}, \\ \psi_n(x) &= \frac{1}{\sqrt{L}} e^{-i\frac{e}{\hbar c} \int_0^x A_1(y) dy - i\frac{\epsilon_n}{\hbar} x}, \end{aligned} \quad (4.1)$$

where ϵ_n is the energy eigenvalues and L is the circumferential length of the zigzag torus: $L = 3a|M|$. We expand the fermion field using the left and right moving waves as

$$\begin{aligned} \Psi(x, T) &= \Psi_L(x, T) + \Psi_R(x, T) \\ &= \sum_{n \in \mathbb{Z}} \left[a_n \psi_n(x) e^{-i\frac{\epsilon_n}{\hbar} T} \begin{pmatrix} 1 \\ 0 \end{pmatrix} + b_n \psi_n(x) e^{+i\frac{\epsilon_n}{\hbar} T} \begin{pmatrix} 0 \\ 1 \end{pmatrix} \right], \end{aligned} \quad (4.2)$$

where a_n, b_n are independent fermionic annihilation operators satisfying the anti-commutators:

$$\{a_n, a_m^\dagger\} = \{b_n, b_m^\dagger\} = \delta_{nm}. \quad (4.3)$$

All the other anticommutator vanish.

In order to get the energy spectrum ϵ_n , we have to impose a boundary condition to the eigenfunctions. We take (2.12) as a general boundary condition. The boundary condition of the zigzag torus in the Y-direction becomes the following:

$$\hat{G}(M(2T_2 - T_1))|\Psi^k\rangle = e^{\pm i\frac{2\pi}{3}\tilde{N}}|\Psi^k\rangle, \quad (4.4)$$

where plus(minus) in exponent has its origin in the two Fermi points, $\tilde{k}_1(\tilde{k}_2)$. Hence we should impose the following boundary conditions on the fermion energy eigenfunctions,

$$\psi_n(x+L) = e^{\pm i\frac{2\pi}{3}\tilde{N}}\psi_n(x), \quad (4.5)$$

then the energy eigenvalues are given by

$$\epsilon_n = \frac{\hbar}{L} \left[2\pi(n \pm \frac{\tilde{N}}{3}) - \frac{e}{\hbar c} \oint_0^L A_1 dy \right]. \quad (4.6)$$

Here, the gauge field A_1 is experimentally controllable by the following experimental setup, see Fig.3. On a planar geometry we set a CNT torus and put some magnetic field inside the CNT torus perpendicular to the plane. In this case the gauge field that expresses this magnetic field is given by, in the vector notation, $A = \frac{N\phi_D}{2\pi}\nabla\theta$ where θ is an angle of two points on the torus. Therefore we get a component,

$$A_1 = \frac{N\phi_D}{L}, \quad (4.7)$$

where $\phi_D = \frac{2\pi\hbar c}{e}$. This vector potential expresses the N flux inside the torus and by tuning the magnetic field, N can be taken as a real number.

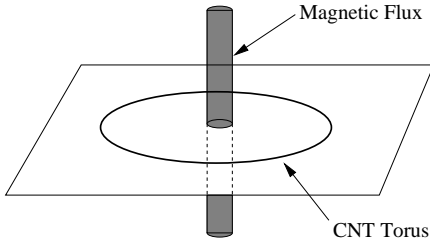


FIG. 3. A CNT torus on a planar geometry with magnetic field

The Lagrangian density (3.8) with chiral fermion has the classical conserved currents

$$j^\mu(x) = \bar{\Psi}(x)\gamma^\mu\Psi(x), \quad (4.8)$$

$$j_5^\mu(x) = \bar{\Psi}(x)\gamma^\mu\gamma^5\Psi(x) = \epsilon^{\mu\nu}j_\nu(x), \quad (4.9)$$

where $\epsilon^{\mu\nu}$ is an antisymmetric tensor: $\epsilon^{01} = 1$. Therefore, the following two charges conserve in the time evolution of the system at the classical level,

$$Q = \oint j^0(x)dx, \quad (4.10)$$

$$Q_5 = \oint j_5^0(x)dx. \quad (4.11)$$

j^μ (electric current) conservation is due to the gauge symmetry and j_5^μ (chiral current) conservation is due to the global chiral symmetry $\Psi \rightarrow e^{i\gamma_5\alpha}\Psi$.

Different from classical mechanics, in the world of quantum mechanics, the chiral symmetry is broken [7]. In order to find what is happening, we analyze the vacuum structure: $|vac; N_L, N_R\rangle = |vac; N_L\rangle \otimes |vac; N_R\rangle$, where

$$|vac; N_L\rangle = \prod_{n=-\infty}^{N_L-1} a_n^\dagger|0\rangle, \quad |vac; N_R\rangle = \prod_{N_R}^{n=\infty} b_n^\dagger|0\rangle. \quad (4.12)$$

We define $|vac; N_L\rangle(|vac; N_R\rangle)$ such that the levels with energy lower than $\epsilon_{N_L}(-\epsilon_{N_R-1})$ are filled and the others are empty. On this vacuum the charge expectation values and the energy become

$$\langle Q \rangle = N_L - N_R, \quad (4.13)$$

$$\langle Q_5 \rangle = N_L + N_R - 2N - 1 \pm \frac{\tilde{N}}{3}, \quad (4.14)$$

$$\langle H_F \rangle = \frac{2\pi\hbar}{L} \left(\frac{\langle Q \rangle^2 + \langle Q_5 \rangle^2}{4} - \frac{1}{12} \right). \quad (4.15)$$

To obtain the above results, we have regularized the divergent eigenvalues on the vacuum by ζ -function regularization, for example, the gauge charge is regularized as follows:

$$Q = \lim_{s \rightarrow 0} \left(\sum_{n \in \mathbb{Z}} a_n^\dagger a_n \frac{1}{|\lambda\epsilon_n|^s} + \sum_{n \in \mathbb{Z}} b_n^\dagger b_n \frac{1}{|-\lambda\epsilon_n|^s} \right), \quad (4.16)$$

where λ is an arbitrary constant with dimension of length which is necessary to make $\lambda\epsilon_n$ dimensionless. This regularization respects gauge invariance because the energy of each level is a gauge invariant quantity.

It can be shown that the gauge charge $\langle Q \rangle$ must vanish in order that the state is a physical state. We now have $N_L = N_R$. From the above equation (4.14), it can be seen that if N_L and N_R are conserved, then, by varying N (the magnetic field), the chiral charge also changes. Therefore it is not a conserved quantity. We thus see that the vacuum is responsible for non-conservation of chirality even though the dynamics is chirally invariant. From eq.(4.9) we see that the chiral current j_5^0 is equivalent to the electric current in the tubule axis direction,

$$Q_5 = \oint j_5^0(x)dx = - \oint j^1(x)dx = -J^1. \quad (4.17)$$

Hence, in order to observe the anomaly, we should observe the electrical current in the torus.

Due to the existence of the two Fermi points, the total current of the torus is given by the sum of two currents $\langle Q_5 \rangle_{\tilde{k}_1}$ and $\langle Q_5 \rangle_{\tilde{k}_2}$. We should care for the sign(\pm) in the chiral charge (4.14). We define

$$\langle Q_5 \rangle_{\tilde{k}_1} = N_L + N_R - 2N - 1 + \frac{\tilde{N}}{3}, \quad (4.18)$$

$$\langle Q_5 \rangle_{\tilde{k}_2} = N_L + N_R - 2N - 1 - \frac{\tilde{N}}{3}, \quad (4.19)$$

and treat them separately.

It is clear from the above equations that there are two origins of the usual current flow along the torus. One is the $N_L + N_R$ term which can be induced in thermal bath or by a sudden change of the magnetic field. On the other hand, magnetic field can change the quantum vacuum structure and lead to the anomaly. In order to avoid the unexpected changes of $N_L (= N_R)$, the magnetic field must be changed adiabatically at low temperature. However, in the adiabatic process, when the strength of the magnetic field reaches the specific points, then $N_L (= N_R)$ also have to change. For simplicity, we set $\tilde{N} = 1$ and focus on the $\langle Q_5 \rangle_{\tilde{k}_1}$. When increasing N starting from the point $N = 0, N_L = 0$, the energy is going up as in eq(4.15). At $N = \frac{1}{6}$, the spectrum meets an another line of spectrum $N_L = 1$, see Fig.4. Therefore the circular current for \tilde{k}_1 in the ring

$$J^1(\tilde{k}_1) = 2(N - N_L) + \frac{2}{3} \quad (4.20)$$

follows the line shown in Fig.5.

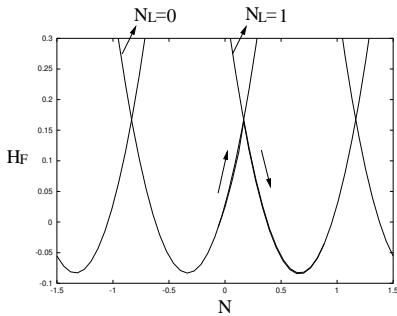


FIG. 4. Adiabatic change of the fermionic energy of \tilde{k}_1 point. The energy value is labeled in the unit of $\frac{2\pi\hbar}{L}$

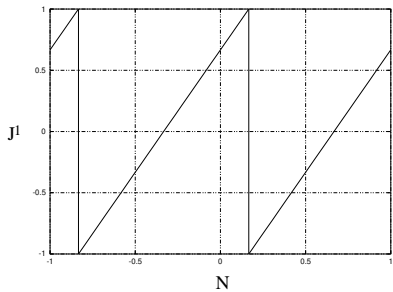


FIG. 5. Induced current in the twisted zigzag torus: $J^1(\tilde{k}_1) = -\langle Q_5 \rangle_{\tilde{k}_1}$

The same analysis can be applied to the case of $J^1(\tilde{k}_2) = -\langle Q_5 \rangle_{\tilde{k}_2}$, the adiabatic change of energy and induced current are shown in Fig.6 and Fig.7.

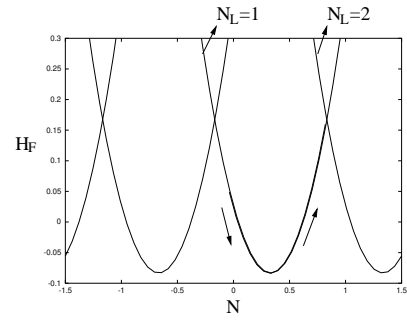


FIG. 6. Adiabatic change of the fermionic energy of \tilde{k}_2 point. The energy value is labeled in the unit of $\frac{2\pi\hbar}{L}$

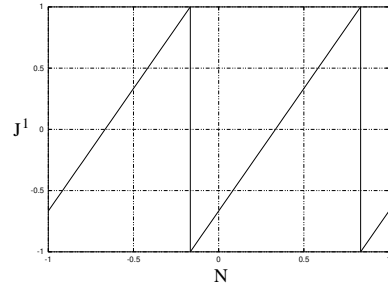


FIG. 7. Induced current in the twisted zigzag torus: $J^1(\tilde{k}_2) = -\langle Q_5 \rangle_{\tilde{k}_2}$

Total current on the torus is given by a sum of two current,

$$J = J^1(\tilde{k}_1) + J^1(\tilde{k}_2). \quad (4.21)$$

Magnetic field dependence of the total current is shown in Fig.8. Dotted line in Fig.8 indicates the current on the untwisted($\tilde{N} = 0$) torus.

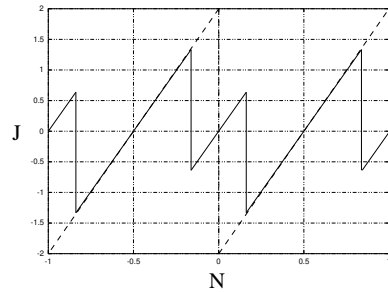


FIG. 8. Magnetic field dependence of the total current on the torus: $J = J^1(\tilde{k}_1) + J^1(\tilde{k}_2)$

V. VACUUM STRUCTURE OF CARBON NANOTUBE TORUS

In this section we consider the vacuum structure of the total Hamiltonian:

$$H = \oint \mathcal{H} = H_F + H_C, \quad (5.1)$$

$$H_C = \frac{e^2}{8\pi c} \oint \frac{J^0(x)J^0(y)}{|x-y|} dx dy.$$

In the previous section we have solved the kinetic part of the total Hamiltonian. We clarified its vacuum state and obtained the regularized eigenvalues of the physical quantities. We saw that the vacuum has the chiral charge so that it read the chiral anomaly. What we are interested in at this point is whether the previous results change or not by the inclusion of the Coulomb interaction in our analysis. Furthermore we hope to make clear the effects of the ‘external’ charge density [8]. Their understandings are the first step for studying more physically interesting situations such as impurity effect, CNT-CNT junction or junctions of a CNT and a metal or a superconductor.

The Coulomb interaction consists of a product of the charge density. Therefore it is very convenient to rewrite the kinetic term H_F using the current operators. For this purpose, it is useful to introduce the left and right currents as follows:

$$J^0(x) = J_L(x) + J_R(x), \quad (5.2)$$

where $J_L(x) = \Psi_L^\dagger(x)\Psi_L(x)$ and $J_R(x) = \Psi_R^\dagger(x)\Psi_R(x)$. We expand these currents by the Fourier modes,

$$J_L(x) = \sum_{n \in \mathbb{Z}} \frac{j_L^n}{L} e^{-i\frac{2\pi n x}{L}}, \quad J_R(x) = \sum_{n \in \mathbb{Z}} \frac{j_R^n}{L} e^{+i\frac{2\pi n x}{L}}, \quad (5.3)$$

where the Fourier components are the bosonic operators,

$$j_L^n = \sum_{m \in \mathbb{Z}} a_m^\dagger a_{m+n}, \quad j_R^n = \sum_{m \in \mathbb{Z}} b_{m+n}^\dagger b_m, \quad (5.4)$$

which satisfy the following commutation relations on the fermion Fock space,

$$[j_L^n, (j_L^m)^\dagger] = n\delta_{n,m}, \quad (5.5)$$

$$[j_R^n, (j_R^m)^\dagger] = n\delta_{n,m}. \quad (5.6)$$

It is well-known that the following Hamiltonian has the same matrix element as the original fermion Hamiltonian:

$$H_F = \frac{2\pi\hbar}{L} \left\{ \left(\frac{Q^2 + Q_5^2}{2} - \frac{1}{12} \right) + \sum_{n>0} ((j_L^n)^\dagger j_L^n + (j_R^n)^\dagger j_R^n) \right\}. \quad (5.7)$$

This Hamiltonian has a new term which is not shown in eq.(4.15). This term has vanishing value on the previous vacuum state because

$$j_L^n |vac; N_L\rangle = 0, \quad j_R^n |vac; N_R\rangle = 0, \quad (5.8)$$

for positive n .

The Coulomb interaction reads,

$$H_C = \frac{e^2}{4\pi L c} \sum_{n \geq 0} V(n) ((j_L^n)^\dagger + j_R^n) (j_L^n + (j_R^n)^\dagger). \quad (5.9)$$

Here, we introduce the Fourier component of the Coulomb potential,

$$V(n) = 2\pi \int_0^1 dz \frac{\cos(2\pi n z)}{\sqrt{\sin^2(\pi z) + \left(\frac{R}{L}\right)^2}}, \quad (5.10)$$

where R is the circumference of the tubule.

Some comments are in order. When we write the Coulomb interaction in eq.(5.1), it has a ultraviolet divergence in the limit of $x \rightarrow y$. Therefore we need to introduce some cutoff length. It is appropriate that we set it the length of a diameter of a tubule because we make the approximation that mixing of the different momentums in the compactified direction cannot happen. This explain the $\left(\frac{R}{L}\right)^2$ term in the denominator. Besides, the form of a torus is not a line but a ring on a plane so that we should use the direct length between x and y in the Coulomb interaction. This is the origin of the $\sin^2(\pi z)$ term in the denominator.

We combine the kinetic term and the Coulomb term as follows:

$$H = H_0 - \frac{2\pi\hbar}{12L} + \sum_{n>0} H_n, \quad (5.11)$$

where

$$H_0 = \frac{2\pi\hbar}{L} \frac{Q_5^2 + \kappa Q^2}{2}, \quad \kappa = 1 + \frac{\alpha}{8\pi^2} V(0), \quad (5.12)$$

and

$$H_n = \frac{2\pi\hbar}{L} \left\{ (j_L^n)^\dagger j_L^n + j_R^n (j_R^n)^\dagger - n \right\} + \frac{e^2 V(n)}{4\pi L c} ((j_L^n)^\dagger + j_R^n) (j_L^n + (j_R^n)^\dagger). \quad (5.13)$$

Here we introduce the fine structure constant $\alpha (= \frac{e^2}{\hbar c})$.

We diagonalize the Hamiltonian $H_n (n \neq 0)$ using the Bogoliubov transformation:

$$\begin{pmatrix} \tilde{j}_L^n \\ (\tilde{j}_R^n)^\dagger \end{pmatrix} = \begin{pmatrix} \cosh t_n & \sinh t_n \\ \sinh t_n & \cosh t_n \end{pmatrix} \begin{pmatrix} j_L^n \\ (j_R^n)^\dagger \end{pmatrix}, \quad (5.14)$$

where

$$\sinh 2t_n = \frac{1}{E_n} \frac{e^2 V(n)}{4\pi L c}, \quad (5.15)$$

$$\cosh 2t_n = \frac{1}{E_n} \left(\frac{2\pi\hbar}{L} + \frac{e^2 V(n)}{4\pi L c} \right), \quad (5.16)$$

$$E_n = \frac{2\pi\hbar}{L} \sqrt{1 + \frac{\alpha}{4\pi^2} V(n)}. \quad (5.17)$$

After some calculations we derive

$$H_n = E_n [(\tilde{j}_L^n)^\dagger \tilde{j}_L^n + (\tilde{j}_R^n)^\dagger \tilde{j}_R^n + n] - \frac{2\pi\hbar}{L}n. \quad (5.18)$$

The energy E_n differs from $\frac{2\pi\hbar}{L}$. The difference is due to the Coulomb interaction and is very small owing to the factor $\frac{\alpha}{4\pi^2}$, see Fig.9.

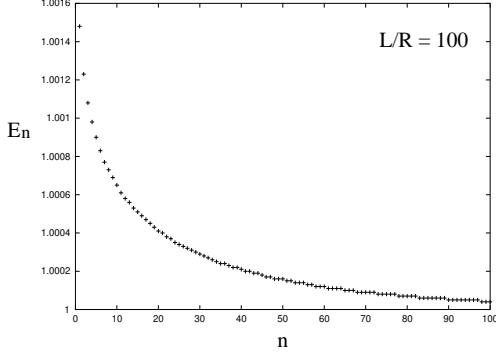


FIG. 9. Energy spectrums are corrected slightly by the Coulomb interaction. The energy value is labeled in the unit of $\frac{2\pi\hbar}{L}$. Here we set $\frac{L}{R} = 10^2$ in eq.(5.10).

The generators of the Bogoliubov transformation are given by

$$U_n = \exp(-t_n \{(\tilde{j}_L^n)^\dagger (\tilde{j}_R^n)^\dagger - \tilde{j}_L^n \tilde{j}_R^n\}). \quad (5.19)$$

Hence, we obtain the vacuum state as follows:

$$|\widetilde{vac}\rangle = \left(\prod_{n>0} U_n \right) |vac; N_L, N_R\rangle, \quad (5.20)$$

where $N_L = N_R$. The previous vacuum state changes into new vacuum by the Coulomb interaction. We should estimate the gauge charge and chiral charge on this new vacuum. Because the operators(U_n) commute with the charge operators Q and Q_5 , the eigenvalues of these charges do not change.

$$Q|\widetilde{vac}\rangle = 0, \quad (5.21)$$

$$Q_5|\widetilde{vac}\rangle = \left(2(N_L - N) - 1 \pm \frac{\tilde{N}}{3} \right) |\widetilde{vac}\rangle. \quad (5.22)$$

Hence, the chiral anomaly which we have considered in the previous section still exists when we include the Coulomb interaction into the analysis.

VI. EFFECTS OF EXTERNAL CHARGES

We have so far considered the Coulomb interaction between the internal charges. However, more important problem may be the following: when we put external charges on a carbon nanotube torus, how the vacuum structure change? A fixed external charge may corresponds to an electrical contact or an impurity on a CNT

torus. In this section we put external charges on a torus and study the vacuum structure. Especially we analyze the potential behavior between a pair of external charges and the ‘charge screening’ effect which means that the internal charge density is induced by the external charges so that the external charges are screened.

We set two unit external charges on a torus. One has a unit charge e placed at x_0 and the other has an opposite charge $-e$ at y_0 .

$$\begin{aligned} J_{ex}^0(x) &= \delta(x - x_0) - \delta(x - y_0) \\ &= \frac{1}{L} \sum_{n \in Z} j_{ex}^n e^{-i \frac{2\pi n x}{L}}, \end{aligned} \quad (6.1)$$

where

$$j_{ex}^n = e^{i \frac{2\pi n x_0}{L}} - e^{i \frac{2\pi n y_0}{L}}. \quad (6.2)$$

We consider the Coulomb interaction with the following charge density which is a sum of the internal charges and the external charges:

$$\begin{aligned} J^0(x) + J_{ex}^0(x) &= \\ \sum_{n \in Z} ((j_L^n)^\dagger + j_R^n + (j_{ex}^n)^*) &\frac{1}{L} e^{+i \frac{2\pi n x}{L}}. \end{aligned} \quad (6.3)$$

After some calculations we get

$$\begin{aligned} H_n = E_n \left[((\tilde{j}_L^n)^\dagger + \gamma_n (j_{ex}^n)^*) (\tilde{j}_L^n + \gamma_n j_{ex}^n) \right. \\ \left. + ((\tilde{j}_R^n)^\dagger + \gamma_n j_{ex}^n) (\tilde{j}_R^n + \gamma_n (j_{ex}^n)^*) + n \right] \\ - \frac{2\pi\hbar}{L}n + \sum_{n>0} \frac{\beta_n}{E_n^2} \left(\frac{2\pi\hbar}{L} \right)^2 (j_{ex}^n)^* j_{ex}^n, \end{aligned} \quad (6.4)$$

where $\gamma_n = \sinh 2t_n (\cosh t_n - \sinh t_n)$ and $\beta_n = \frac{e^2}{4\pi L C} V(n)$. It is easy to find conditions of the vacuum in the presence of the external charges,

$$(\tilde{j}_L^n + \gamma_n j_{ex}^n) |\widetilde{vac}; J_{ex}^0\rangle = 0, \quad (6.5)$$

$$(\tilde{j}_R^n + \gamma_n (j_{ex}^n)^*) |\widetilde{vac}; J_{ex}^0\rangle = 0. \quad (6.6)$$

We estimate the energy change due to the presence of the external charges:

$$\begin{aligned} E(x_0 - y_0) &= \langle \widetilde{vac}; J_{ex}^0 | H | \widetilde{vac}; J_{ex}^0 \rangle - \langle \widetilde{vac} | H | \widetilde{vac} \rangle \\ &= \sum_{n>0} \frac{\beta_n}{E_n^2} \left(\frac{2\pi\hbar}{L} \right)^2 (j_{ex}^n)^* j_{ex}^n \\ &= \frac{2\pi\hbar}{L} \sum_{n>0} \frac{\frac{\alpha}{4\pi^2} V(n)}{1 + \frac{\alpha}{4\pi^2} V(n)} \left(1 - \cos \frac{2\pi n(x_0 - y_0)}{L} \right). \end{aligned} \quad (6.7)$$

This energy may be approximated by

$$E(x_0 - y_0) \simeq \frac{\alpha}{4\pi} \frac{2\pi\hbar}{R} \left(1 - \frac{1}{\sqrt{1 + \left(\frac{\pi(x_0 - y_0)}{R} \right)^2}} \right). \quad (6.8)$$

Fig.10 shows the potential energy (eq.(6.7)) as a function of the distance between the two external charges.

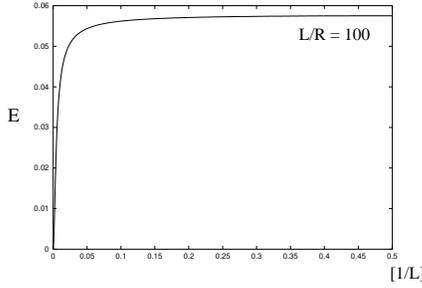


FIG. 10. Distance dependence of the energy caused by two fixed external charges. The energy value is labeled in the unit of $\frac{2\pi\hbar}{L}$. The distance between two external charges is scaled by L . Here we take $\frac{L}{R} = 10^2$ in eq.(5.10).

We see that the effect of the ‘charge screening’ on the external charge can be ignored in a metallic carbon nanotube torus. Because the potential energy is now shown to be long-ranged. This means that even if some internal charges are influenced by the external charges, the quantity of the induced charges should be very small. To confirm this, we also compute the induced internal charges distribution,

$$\langle \widetilde{vac}; J_{ex}^0 | J^0(x) | \widetilde{vac}; J_{ex}^0 \rangle = f(x; x_0) - f(x; y_0), \quad (6.9)$$

where

$$f(x; x_0) = -\frac{1}{L} \frac{\frac{\alpha}{4\pi^2} V(0)}{1 + \frac{\alpha}{4\pi^2} V(0)} - \frac{2}{L} \sum_{n>0} \frac{\frac{\alpha}{4\pi^2} V(n)}{1 + \frac{\alpha}{4\pi^2} V(n)} \cos \frac{2\pi n(x - x_0)}{L}. \quad (6.10)$$

This function is displayed in Fig.11. It is clear that the induced charge density is very small. Hence, the charge screening effect is incomplete.

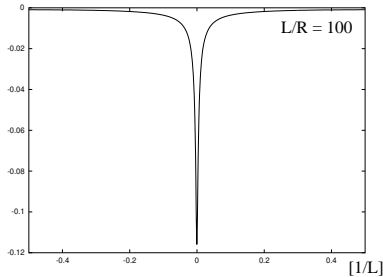


FIG. 11. The internal charge density modulation around a unit charge e placed at origin: $f(x, 0)$. The charge density value and the distance from the charge are labeled in the unit of $\frac{1}{L}$.

VII. CONCLUSION AND DISCUSSION

In this paper we analyzed the carbon nanotube torus and discussed the quantum mechanical vacuum structure of a metallic carbon nanotube torus. The significance of our present work may be put as follows.

We used the quantum field theory to analyze the vacuum structure of a metallic CNT torus. We pointed out that the chiral anomaly in 1+1 dimensions should be observed in an appropriate experimental setting. We also clarified the vacuum state including the Coulomb interaction and discussed the effect of ‘charge screening’ on the external charges. It was found that the charge screening effect is negligibly small. This is to be contrasted with the screening effect for the massless Schwinger model [8].

Although we have analyzed CNT torus in the present paper, we can regard the torus as a tube locally provided the circumferential length of the torus is large. Hence, we may apply the results obtained in the analysis of the torus to a study of carbon nanotube. To take an example, it is reasonable to suppose that the screening effect is also negligible on a tube like a torus.

What we do not consider in this paper are effects of finite temperature on chiral anomaly and screening of external charges on a CNT torus. In finite temperature, in addition to the electron field, phonon field would come into play [15]. This phonon field may be vital to understand the electrical behavior of the carbon nanotube at finite temperature. We would like to make a quantitative analysis of finite temperature effects in a future report.

VIII. ACKNOWLEDGMENTS

The author would like to thank M. Hashimoto for various discussions on the subject. This work is supported by a fellowship of the Japan Society of the Promotion of Science.

-
- [1] S. Iijima, *Nature*, **354**, 56(1991).
 - [2] R. Saito, G. Dresselhaus and M.S. Dresselhaus, *Physical Properties of Carbon Nanotubes* (1998) Imperial College Press, London.
 - [3] *The Science and Technology of Carbon Nanotubes* (1999) Ed. by K. Tanaka, T. Yamabe and K. Fukui, Elsevier Oxford.
 - [4] J.W. Mintmire, B.I. Dunlap and C.T. White, *Phys. Rev. Lett.* **68**, 631 (1992); N. Hamada, S. Sawada and A. Oshiyama, *Phys. Rev. Lett.* **68**, 1579 (1992); R. Saito, M. Fujita, G. Dresselhaus, and M. Dresselhaus, *Appl. Phys. Lett.* **60**, 2204 (1992).
 - [5] J. W. G. Wildöer et al. *Nature*, **391**, 59 (1998); T. W. Odom, J. L. Huang, P. Kim and C. M. Lieber, *Nature*, **391**, 62 (1998).
 - [6] J. Liu et al. *Nature*, **385**, 781(1997).
 - [7] J.S. Bell and R. Jackiw, *Nuovo Cim.* **60**, 47(1969); S. Adler, *Phys. Rev.* **177**, 2426(1969).
 - [8] S. Iso and H. Murayama, *Prog. Theor. Phys.* **84**, 142(1990)

- [9] J. González, F. Guinea and M.A.H. Vozmediano, Nucl. Phys. **B406**, 771 (1993).
- [10] Y. -K. Kwon and D. Tománek, Phys. Rev. B. **58**, R16001 (1998).
- [11] W. Clauss, D. J. Bergeron and A. T. Johnson, Phys. Rev. B. **58**, R4266 (1998).
- [12] It should be noted that to obtain eq.(2.20) we have to perturb the Hamiltonian around the points $\tilde{k}_1 - a\tilde{K}_1$ and $\tilde{k}_2 + a\tilde{K}_1$. The wave vectors K_i satisfy the conditions, $K_i \cdot T_j = 2\pi\delta_{ij}$. The vectors $\tilde{k} \pm a\tilde{K}_1$ and \tilde{k} represent the same state since any two wave vectors congruent by $a\tilde{K}_i$ are just different labels of the same state.
- [13] J. C. Slonczewski and P. R. Weiss, Phys. Rev. **109**, 272 (1958).
- [14] In order to get the unnormalized energy we should multiply β by ϵ_n . We estimate the order of magnitude of energy spectrum using $\beta \sim \frac{c}{400}$. Here we use $\gamma = 2.5[\text{eV}]$ (This value should depend on the temperature) and $a = 1.5[\text{\AA}]$,

$$\beta\epsilon_n = 5(\text{eV}) \left[\frac{\text{\AA}}{L} \right] 2\pi (n - N).$$
- [15] B. Sakita and K. Shizuya, Phys. Rev. B. **42**, 5586 (1990).